Proceedings of the XXVIII International Mineral Processing Congress, September 11-15 2016, Québec City, Canada

Keynote Paper No. 603: Lightweight Metals and Composites: Production, Processing and Applications

DEVELOPMENT OF ADVANCED TITANIUM ALLOYS FOR AEROSPACE, MEDICAL AND AUTOMOTIVE APPLICATIONS

*C. Siemers[1], F. Brunke[1], K. Saksl[2], J. Kiese[3], M. Kohnke[1], F. Haase[1], M. Schlemminger[1], P. Eschenbacher[1], J. Fürste[1], D. Wolter[4], H. Sibum[5]

[1]Technische Universität Braunschweig
Institut für Werkstoffe
Langer Kamp 8
38106 Braunschweig, Germany
*(*Corresponding author: c.siemers@tu-bs.de)*

[2]Slovak Academy of Sciences
Institute of Materials Research
Watsonova 47
04353 Kosice, Slovak Republic

[3]VDM Metals GmbH
Westendstrasse 15
45143 Essen, Germany

[4]Osteosynthese-Institut GbR
Roggenweg 8
22926 Ahrensburg, Germany

[5]Ingenieurbüro für Werkstoffverarbeitung und –design
Am Busch 10
41515 Grevenbroich, Germany

ABSTRACT

In general, titanium alloys combine outstanding mechanical properties with corrosion resistance and biocompatibility and are, therefore, used in many challenging applications. Nevertheless, for special products, well-tailored properties are required which might not be achievable by a specific design so that new or modified alloys are needed. In this overview paper, alloy development strategies performed at the Institute for Materials of the Technische Universität Braunschweig are discussed at different examples, namely, (1) oxidation-resistant, microstructural-stabilized and cold-workable alloys for exhaust applications, (2) aluminum- and vanadium-free, medium-strength and cold-workable alloys for implants and osteosynthesis applications and (3) free-machining alloys by the addition of particles with low melting points for non-safety critical light-weight constructions to replace heavier steels, e.g. in automotive applications. A special focus is set on the alloy development techniques and the analyses carried out to achieve well-balanced properties by the optimization of the alloy compositions.

KEYWORDS

Titanium, CP-Titanium, titanium alloys, alloy development, oxidation resistance, oxidation resistant titanium alloys, medical applications, free-machining titanium alloys

INTRODUCTION

Titanium belongs to the allotropic metals and can therefore exist in two different equilibrium lattice modifications. Pure titanium crystallizes at 1668°C in a body centered cubic (bcc) structure called β-titanium which at 882°C transforms to a hexagonal close packed structure (hcp), the α-titanium. A martensitic β-to-α-transformation is possible at large cooling rates. This thermally induced hexagonal martensite is called the α'-phase. The transformation temperature named β-transus-temperature (T_β) can be influenced by alloying elements (Peters & Leyens, 2002).

For titanium alloy production typical alloying elements are aluminum (Al) and oxygen (O), both α-stabilizers shifting the β-transus temperature to higher temperatures, whereas tin (Sn) and zirconium (Zr) only show a limited influence on the β-transus temperature. The β-stabilizing elements are subdivided into two groups: Niobium (Nb), molybdenum (Mo) and vanadium (V) stabilize the β-phase between the melting point and room temperature and are therefore called isomorphous β-stabilizers. Elements like copper (Cu), iron (Fe) or silicon (Si) also stabilize the β-phase to lower temperatures but undergo a eutectoid reaction during cooling. β-titanium then dissociates to α-titanium and an intermetallic compound. Consequently, these elements are called eutectoid β-stabilizers (Boyer, Welsh & Collings, 1994).

According to the phases present at room temperature, titanium alloys are divided into four main groups, namely CP-Titanium (commercially pure titanium, containing low amounts of oxygen, iron, nitrogen and carbon), consisting of nearly 100% α-phase. α- and near-α-alloys are composed of α-phase and up to 5% of β-phase at room temperature. Near-β- and β-alloys on the other hand contain more than 95% of β-phase (Peters & Leyens, 2002). Finally, there are the two-phase alloys containing between 5% and 95% β-phase at room temperature. They are divided into two subgroups: In (α+β) alloys a (partial) martensitic transformation is possible, whereas in metastable β-alloys the martensite start temperature lies below room temperature. After water quenching, metastable β-alloys consist of β-phase only, the so-called supercooled metastable state (Donarchie, 1988). Ageing of supercooled β-phase leads to the formation of α-phase and the metastable ω-phase in some alloys (Ng, Douguet, Bettles & Muddle, 2010). Hence, metastable β-alloys can be precipitation hardened to ultimate tensile strengths up to 1400 MPa (Lütjering & Williams, 2007).

During the industrial titanium alloy production, titanium sponge coming from Kroll's process is mixed with alloying elements and compressed to parts (Peters & Leyens, 2002). The resulting compacts are welded together to form an electrode. The electrodes are molten to a first ingot in a vacuum arc furnace (VAR). To ensure sufficient homogeneity of the alloy, the first ingot has to be remolten once for standard applications or twice for safety critical applications, e.g. compressor discs of aircraft engines. For first ingot production, nowadays, electron beam cold hearth remelting (EBCHR) is used, especially for non-safety critical applications (Okano, Hatta, Tada & Tanaka, 2007). Independent of the melting procedure, the final ingots are normally deformed by forging, rotary swaging, rod extrusion or rolling to form bars, rods, plates or sheets (Peters & Leyens, 2002). If the thermo-mechanical treatments are performed in air, oxygen can diffuse into the surface. As oxygen is a strong α-stabilizer, here a partial transformation to α-phase can occur, the so-called α-case formation. Along with the phase transformation, increased hardness, reduced toughness and notch-sensitivity are observed in the α-case due to the interstitially dissolved oxygen. Therefore, the α-case is normally removed by stripping or grinding before any application of the semi-finished products (Lütjering & Williams, 2007).

Titanium's Behavior at Elevated Temperature and Requirements for Exhaust Applications

Much of the cost related to titanium products stem from the difficulty in reducing the oxide into a metal, but once purified, titanium is resistant to re-oxidation on account to a thin TiO_2 layer which forms spontaneously when a metallic titanium surface is exposed to air (Foy & Yu, 2012). However, at temperatures above 550°C, this oxidation resistance is dramatically lost. This can be explained by a partial transformation of TiO_2 to TiO_2 and Ti_2O_3, producing additional phase boundaries and lattice mismatches.

In addition, this leads to the presence of Ti^{4+} and Ti^{3+} ions and, hence, to vacancies in the oxygen sublattice of the oxide layer. Both effects support accelerated oxygen diffusion through the oxide layer (Lütjering & Williams 2007). Consequently, at the metal-oxide interface, additional oxidation occurs leading to a volume increase so that the oxide layer finally peels off and the process starts again. The poor oxidation resistance hinders the application of titanium alloys in high temperature environments, e.g. in the high pressure compressor of aircraft engines, in turbine applications or for exhaust systems, for which they are otherwise very well suited (Peters & Leyens, 2002).

Considerable efforts have been made since the late 1980ies to improve the oxidation resistance of conventional titanium alloys at elevated temperature. Besides large amounts of aluminum so that an Al_2O_3 layer forms the two most effective elements are silicon and niobium (Maki, Shioda, & Sayashi, 1992). In case of silicon, this can be explained by (1) the formation of a thin SiO_2-layer at the metal-oxide interface forming a diffusion barrier for oxygen penetration and thus reducing further oxidation and (2) the precipitation of Ti_3Si intermetallic phase at the grain boundaries decelerating grain boundary oxidation (Lütjering & Williams, 2007). Since niobium forms a pentavalent oxide, it is believed that the effect is due to Nb^{5+} ions in the oxide. It was proposed that Nb^{5+} ions diffuse into the metal sub-lattice of the oxide (TiO_2) compensating the presence of Ti^{3+} ions which in turn trap the oxygen vacancies. Other suggested causes are the formation of Nb_2O_5 or one of the different niobium nitrides at the metal-oxide-interface, the involvement of other elements like aluminum and nitrogen, or the formation of mixed oxides (Lütjering & Williams, 2007). Finally, the formation of a niobium-rich layer below the α-case hindering the oxygen diffusion into the titanium matrix was proposed (Tegner, Zhu, Siemers, Saksl & Ackland, 2015).

In general, in titanium alloys grain growth is observed if they are exposed to elevated temperature for longer times. Severe grain growth occurs in the single-phase state, either during heat treatments of any alloy above their β-transus-temperature or if single-phase alloys are annealed above approx. 650°C. Grain growth is a very critical feature in α-alloys as the hexagonal lattice cell shows anisotropic properties. In exhaust applications, normally, sheet materials are applied with wall thicknesses smaller than 2 mm. In case grain growth occurs, only a few grains might be present over the wall thickness after long-time runs at elevated temperatures leading to direction-dependent mechanical properties in the parts (Peters & Leyens, 2002). To prevent grain growth, the above mentioned grain boundary titanium silicides can be used even if a slight embrittlement has to be accepted (Lütjering & Williams, 2007).

For sheet production (as needed for exhaust applications), ingots coming from VAR or slabs produced by EBCHR are normally hot rolled first (Boyer & Williams, 2012). Afterwards the final reduction in thickness is produced by cold rolling followed by recrystallisation to achieve a fine-grained microstructure. Oxidation resistant, mainly α-phase containing titanium alloys normally do not show good cold-workability due to (1) the α-cell itself with its relatively low c/a ratio which only has three independent slip systems and thus reduced deformability and (2) the presence of silicon enhancing the formation of grain boundary titanium-silicides and embrittlement in related alloys (Lütjering & Williams, 2007).

Titanium alloys used in exhaust applications should, therefore, be oxidation-resistant, microstructural-stabilized and cold-workable.

Requirements for Medical Applications

For implant materials, a high specific static strength as well as a superior fatigue limit and a low Young's modulus in combination with corrosion resistance and biocompatibility are required (Lütjering & Williams 2007). Therefore, α- or (α+β)-titanium alloys like CP-Titanium Grade 2 and CP Titanium Grade 4, Ti 6Al 4V and Ti 6Al 7Nb are used for osteosynthesis or implant applications for several decades now and have replaced stainless steels and cobalt-based alloys (Peters & Leyens, 2002).

Although titanium alloys exhibit excellent mechanical properties, corrosion resistance and biocompatibility, disadvantages exist during medical applications. In the recent years, the use of some of

the alloying elements was intensively discussed because of their potential negative effects on the health. It is well known that vanadium as well as its oxides are cytotoxic. The interaction of aluminum with the human body was investigated in several studies (Geetha, Singh, Asokamani& Gogia, 2009). Higher aluminum concentrations in the brain can lead to dementia. In addition, there are ongoing discussions about the fact that aluminum might also cause breast cancer and the Alzheimer's disease (Yokel, Allen, & Ackley, 1999). After surgeries and implantations inflammations might occur. In this case, H_2O_2 can be released which in turn can remove the TiO_2-layer of titanium implants. Unless the oxide layer has fully recovered, metallic ions (e. g. aluminum in aluminum containing alloys) can infiltrate the blood circuit (Mabilleau, Bourdon, Joly-Guillou, Filmon, Baslé & Chappard, 2006).

Hence, advanced titanium alloys for medical applications should either contain elements that are already present in the human body like oxygen or carbon or for which negative effects on the biocompatibility have not been reported yet, e.g. gold, molybdenum, niobium or silicon. The use of aluminum and vanadium should be excluded as its interaction with the human body is at least unclear. In addition, the mechanical properties, i.e. the tensile strength and the ductility, should be as close as possible to that of Ti 6Al 4V ELI.

Machinability and Chip Formation

The relatively high cost of titanium alloy components limits their use in mass product applications e.g. in the automotive industry. Therefore, in these applications heavier steels have to be used even if CO_2-emissions could be reduced by using lighter titanium constructions. The high component price is a result of the intrinsic raw material costs of titanium, manufacturing costs to produce a semi-finished part and the machining costs incurred to obtain the final shape of the product. Especially, machining of titanium alloys can mean about 50% of the product costs (Tönshoff & Hollmann, 2005).

Machining of titanium alloys is difficult because of their poor machinability. This difficulty arises from the physical, chemical and mechanical properties of titanium (Lütjering & Williams, 2007). In addition, machining operations like drilling and turning in many cases cannot be automated due to the formation of long chips which wrap around the tools (Siemers, Laukart, Zahra, Rösler, Spotz & Saksl, 2010). Therefore, the cutting process has to be interrupted as often as it is necessary to remove the chips from the process zone by an operator as otherwise the finished surfaces and/or the tools might be destroyed. In titanium machining, three different kinds of chips are known to form: continuous chips having a constant chip thickness over the chip's length, segmented chips showing a saw-tooth like structure and completely separated segments if extreme cutting conditions are applied (Hou & Kommanduri, 1997; Obikawa, Anzai, Egawa, Narutaki, Shintani & Takeoka, 2011).

Extended machining studies at more than twenty different titanium alloys applying orthogonal as well as standard cutting operations have been carried out. A wide range of cutting speeds, cutting depths and feed rates has been applied (Siemers et al., 2010; Siemers, Jencus, Baeker, Roesler & Feyerabend, 2007). It could be demonstrated that titanium alloys containing high amounts of α-phase (like CP-Titanium Grades 2 and 4, α- and near-α-, ($\alpha+\beta$)- as well as aged metastable β-alloys) form segmented chips for almost all machining processes and for a wide range of cutting speeds and cutting depths. Solution treated metastable β- as well as near-β- und β-alloys on the other hand show a cutting parameter dependent change in the chip formation process from continuous to segmented chips (Siemers, Laukart, Roesler, Rokicki & Saksl, 2011).

In case of segmented chip formation in titanium alloys, the process starts with damming of the material in front of the tool tip. During further progress of the tool, the deformation in the primary shear zone (a small area leading from the tool tip to the uncut surface) localizes (Healy, Koch, Siemers, Mukherji & Ackland, 2015). Finally, a segment is formed by shear deformation along a shear plane forming a so-called adiabatic shear band with a width of a few micrometers. During the shear band formation in titanium alloys local temperatures can raise to more than 1000°C, the plastic deformation can easily exceed 800%.

The segment formation process itself is driven by a dynamic deformation and recrystallisation process, crack formation has not been observed in any of the experiments (Siemers et al., 2010).

Free-machining titanium alloys should, therefore, produce frgmented chips during machining.

Titanium Research at Technische Universität Braunschweig

Titanium research at the Institute for Materials of the Technische Universität Brausnchweig is focused on alloy development including (1) the production of oxidation-resistant, microstructural-stabilized and cold-workable alloys for exhaust applications, (2) aluminum- and vanadium-free, medium-strength and cold-workable alloys for implants and osteosynthesis applications and (3) free-machining alloys by the addition of particles with low melting points for non-safety critical light-weight constructions to replace heavier steels. In the present paper, an overview about these three alloy development strategies and the related results is given.

EXPERIMENTAL PROCEDURES

Alloy Production

Alloy production has been carried out in a laboratory-size plasma-beam cold-hearth melting facility (PBCHM) with a capacity of approx. 400 grams titanium. Contamination of the alloys during melting was minimized as the PBCHM chamber has been evacuated twice to 2×10^{-5} mbar and flushed with argon (99.999%) in between. Alloy production was carried out in argon atmosphere at a pressure of 600 mbar (argon 99.999%). After melting, turning the ingot and three times remelting, the alloys were cast into a water-cooled copper crucible. The resulting round bars of diameter 13.2 mm and a length of approx. 80 mm have been stress relief annealed to release possible residual stresses from the casting process in an inert gas (argon purity 99.998%) furnace at 700°C ± 10°C for one hour followed by furnace cooling. Afterwards the bars were rotary swaged to a final diameter of 10 mm and turned to safely remove possible contaminated layers and sectioned to approx. 10 mm height by disc cutting.

Larger quantities (approx. 6 kilograms) of alloys have been produced by cold-wall vacuum induction melting and casting at Access in Aachen, Germany. The round bars of approx. 40 mm diameter and a length of 500 mm have been hot rolled at the BTU Cottbus in Cottbus, Germany, to a final height of 6 mm followed by recrystallisation treatments. Industry-size ingots (approx. 4 metric tons) were produced at VDM Metals GmbH in Essen, Germany and have been hot- and cold rolled to a final thickness of 1.2 mm followed by a recrystallisation treatment.

Microstructural Investigations

All samples were embedded into EpoMet® amorphous, glass fiber reinforced polymer by warm embedding at 180°C, 200 bar, for 10 minutes followed by water cooling. Cross sections were prepared by water-cooled mechanical grinding with SiC grinding papers (size P240, P400, P600, P800, P1200 and P2500) and polishing (9 µm, 6 µm, 3 µm, Kulzer NewLam® diamond suspension including lubrication and OPS + H_2O_2 + distilled water). Finally, etching has been carried out using Kroll's reagent (6 ml HNO_3, 3 ml HF, 100 ml H_2O) for 7 to 15 seconds. The morphology of the oxide layer and the microstructure have been analyzed by means of optical microscopy (ZEISS Imager.M2m) and scanning electron microscopy (Hitachi TM 3000, LEO 1550 and FEI Helios Nanolab 650).

Phase analyses have been performed by synchrotron radiation at beamline P07 of PETRA III, DESY (Schell, King, Beckmann, Ruhnau, Kirchhof, Kiehn, Mueller & Schreyer, 2009). Here, even small phase volume fractions (less than 0.5%) can be detected. Two different energies (84.40 keV and 98.50 keV) were used, resulting in wavelengths of 0.01462 nm and 0.012587 nm. The area of exposure was 0.5 mm x 0.5 mm. Samples up to 10 mm thickness have been analyzed in transmission (Debye-Scherrer configuration). The patterns were recorded using a Perkin Elmer 1621 detector, ten shot

averaging. The related phases have been identified using the fit2D (Hammersley, Svensson, Hanfland, Fitch & Häusermann, 1996) and CMPR (Toby, 2005) software.

Investigation of Oxidation, Mechanical Properties and Machinability

Oxidation experiments have been carried out in a standard furnace at 800°C ± 10°C in air for 16, 24, 48, 72, 96 and 288 hours. Three samples of each alloy have been used for any individual condition. The samples were positioned in special Al_2O_3 containers with minimized contact to the metal surface so that contamination of the specimens, e.g. by chemical reactions between the metal and the crucible, could be diminished. In addition, it was ensured that even if parts of the oxide layer peeled off during the oxidation experiments most of the fragments were collected and scaled together with the sample to measure the accurate weight gain. Before the oxidation experiments, the surface area of all samples has been calculated from the height and the diameter (measured at three different positions by means of a micrometer gauge, accuracy 0.01 mm). All specimens have been scaled for three times on precision scales (accuracy 0.1 mg), oxidized and afterwards rescaled to measure the weight gain during oxidation. Due to systematic errors in the volume determination, the overall accuracy of the weight gain measurements was about 10% even if the standard deviation of the individual experiments was much smaller.

The Vickers hardness has been investigated at embedded cross sections of the alloys to get a first approximation of the strength of the alloys. Standard room temperature tensile tests have been carried out according to DIN 50152 (geometry of specimens) and DIN EN ISO 6892-1 (test procedure).

The machinability of the alloys has been investigated in straight turning experiments on a computer numerically controlled lathe. State-of-the-art cutting conditions have been used for all cutting experiments: The cutting speed has been varied between 40 m/min and 80 m/min, two different depths of cut (0.5 mm and 1 mm) have been applied at a fixed feed rate of 0.1 mm/rev.

OXIDATION-RESISTANT, MICROSTRUCTURAL-STABILIZED AND COLD-WORKABLE TITANIUM ALLOYS FOR EXHAUST APPILCATIONS

As the requirements in exhaust systems regarding the mechanical properties are relatively low, all alloys were based on CP-Titanium Grade 1S (soft grade) to ensure good ductility. The use of β-alloys in air at elevated temperature is not advisable as their oxidations resistance is poor compared to that of α- or near-α-alloys (Peters & Leyens, 2002). The deformation characteristic of titanium alloys is a critical feature for exhaust applications. Hence, to avoid solid solution hardening in our α-alloys and to reduce the overall alloy costs, the amount of alloying elements should be kept as low as possible.

Oxidation resistance should be achieved by a concerted addition of niobium, silicon and iron. In earlier experiments, it has been discovered that an iron-silicon ratio of approx.1:4 leads to better oxidation behavior compared to alloys in which silicon has been used without iron addition. This might be due to the fact that iron enhances the diffusion rate of silicon in α-titanium, but the exact mechanism has not been discovered yet.

Microstructure stabilization should be attained by the formation of nano-scale particles distributed mainly on the grain boundaries. As the formation of titanium-silicides reduces the ductility of related titanium alloys, hafnium has been used for several reasons: (1) Hafnium silicides are thermodynamically stable so that dissolution of such particles during long-term application is unlikely even at temperatures above 800°C, (2) the affinity of hafnium to silicon is high so that these silicides should form before titanium-silicides develop and (3) embrittlement of titanium alloys by hafnium-silicides has not been reported so far.

Taking into account all the considerations made in the previous paragraphs, possible compositions of the new class of oxidation-resistant, microstructural-stabilized and cold-workable titanium alloys are Ti (0.05 - 0.4)Si (0.02 - 0.1)Fe (0.01 - 0.5)Nb (0.01 - 0.5)Hf. In particular, the following compositions have

been investigated: Ti 0.4Si 0.1Fe 0.1Hf, Ti 0.4Si 0.1Fe 0.2Hf, Ti 0.4Si 0.1Fe 0.1Nb 0.1Hf and Ti 0.4Si 0.1Fe 0.25Nb 0.1Hf. CP-Titanium Grade 2 was used as reference material.

Microstructure and Phase Composition

After melting and casting, a fully martensitic α'-microstructure developed in the alloys as expected. In the stress-relief annealed state they consisted of α-lamellae; in addition, the former β grain boundaries were visible. The average grain size was about 250 µm. In case of the rolled material the microstructure consisted of equiaxed α-grains and the average grain size was approx. 120 µm. Even in high-resolution SEM imaging, no precipitations have been observed.

The following results were obtained in the synchrotron radiation analyses: All alloys consisted of α-phase, β-phase or titanium-silicides have not been found in any of the alloys. In addition, in all hafnium containing alloys small and broad peaks have been observed which could be related to Hf_5Si_3 intermetallic phase. A Rietveld analyses was not successful due to the low peak-to-background ratio. Nevertheless, the peak shape of Hf_5Si_3 phase indicated the presence of nano-sized precipitations in low amounts.

No grain growth has been observed in any of the hafnium containing alloys after heat treatments at 800°C for 288 hours, once more indicating the presence of thermodynamically stable precipitations located on the grain boundaries. Severe grain growth (the final grain size was larger than 1 mm) occurred in CP-Titanium Grade 2.

Weight Gain during Oxidation and Oxide Layer Morphology

The weight gain of all modified alloys during the oxidation experiments was less than 16 $mg \cdot cm^{-2}$ after 288 hours of oxidation at 800°C. The oxidation followed a parabolic growth law (growth exponent $n \approx 0.5$, diffusion driven oxidation). For Ti 0.4Si 0.1Fe 0.25Nb 0.1Hf the weight gain based growth constant K_p has been calculated to $K_p \approx 6 \cdot 10^{-9}\ kg^2 \cdot m^{-4} \cdot s^{-1}$. The weight gain during the oxidation of CP-Titanium Grade 2 was of more than one order higher compared to the modified alloys and the growth exponent n was close to 1 indicating a linear oxide layer (direct oxygen contact at the oxide-metal-interface) growth.

Metallographic investigations of the oxidized samples showed a dense and crack-free oxide layer with good adhesion to the metal matrix. The oxide layer thickness of Ti 0.4Si 0.1Fe 0.25Nb 0.1Hf was 57 µm after 288 hours of oxidation at 800°C. In contrast to this, the oxide layer of CP-Titanium Grade 2 consisted of interrupted layers with cracks and parts of the oxide layer peeled off. Therefore, only a lower limit of the oxide layer thickness of 200 µm could be measured.

Industrial Scale-Up

Industrial scale-up of the alloy production has been successfully performed. An ingot of four metric tons of the alloy Ti 0.4Si 0.1Fe 0.05Nb 0.1Hf has been produced by vacuum arc remelting; the resulting round bar of diameter 960 mm has been hot forged and stripped to a 3.5 metric tons slab which has been hot-rolled to a thickness of 4.8 mm followed by cold rolling to 1.2 mm and recrystallisation anneal. The microstructure consisted of equiaxed α-grains, see Figure 1, left.

Erichsen cupping experiments (according to DIN EN ISO 20482) showed excelled deformability (impact depth of more than 11 mm) of the alloy, the oxidation resistance of the alloy was even better compared to Ti 0.4Si 0.1Fe 0.25Nb 0.1Hf ($K_p \approx 2 \cdot 10^{-9}\ kg^2 \cdot m^{-4} \cdot s^{-1}$) and the microstructure remained stable due to the presence of Hf_5Si_3 particles, see figure 1, right.

The alloy is now available for exhaust applications for minimum 800°C. First oxidation experiments at 900°C indicate that the application temperature might be even higher.

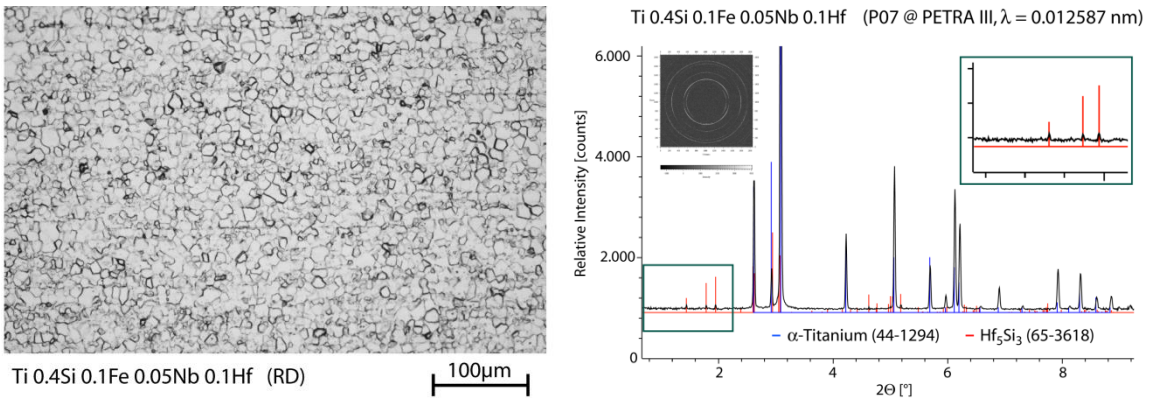

Figure 1 – Left: Microstructure of a forged and cold-rolled 3.5 t ingot of a titanium alloy rolling direction for exhaust application. Right: Phase analyses by synchrotron radiation. Microstructure stabilization is achieved by Hf_5Si_3 precipitates.

ALUMINUM- AND VANDIUM-FREE TITANIUM ALLOYS FOR MEDICAL APPLICATIONS

The following criteria have been applied to identify feasible alloy compositions: (1) First of all, alloying elements that are already present in the human body in larger amounts should be used for strengthening. (2) It is known that elements might get toxic in large concentrations even if they are regarded as uncritical in smaller amounts (Hench & Polak, 2002). So the overall amount of alloying elements (besides the elements mentioned in (1)) should be kept as low as possible. (3) Alloying elements with higher melting temperatures will increase the costs of alloy production, as in our case aluminum containing master alloys which are typically used in titanium alloy production cannot be used. Hence, the amount of molybdenum and niobium should be minimized. (4) A well-balanced strength-to-ductility ratio should be achieved. The yield strength (YTS) should reach or exceed 795 N/mm^2, the ultimate tensile strength (UTS) should be greater than 860 MPa and the elongation at rupture must reach 10%, the minimum values specified for Ti 6Al 4V ELI in ASTM F136. (5) Room-temperature bending of e.g. bone plates should be possible to allow slight bending during surgery of bone fractures to adapt the plate to the bone. Therefore, good ductility is required.

Following these five design criteria, alloy development started with CP-Titanium Grade 4. To increase its strength, oxygen, carbon and iron have been added as these are non-toxic elements which are present in the human body in larger amounts. The nitrogen content remained unchanged (and low) to avoid the formation of titanium nitrides during industrial alloy production, the so-called low-density inclusions. The hydrogen content has not been increased as well to minimize hydrogen induced embrittlement and/or titanium hydride formation.

It is known that especially higher amounts of interstitials lead to embrittlement of titanium alloys so that the carbon and oxygen contents should be kept below a critical limit. Therefore, a preliminary study at binary Ti-O-, T-C- and Ti-Fe-alloys has been carried out to discover feasible oxygen (<0.6%), carbon (<0.2%) and iron (<1.5%) contents. These limits have been identified by microstructural investigations (criterion: no formation of oxides, carbides or intermetallic compounds in related alloys), rotary swaging experiments (criterion: surface crack formation during deformation must not occur) and by notched bar impact tests at different temperatures (criterion: similar impact energies compared to Ti 6Al 4V ELI). Additional elements, i.e. gold, molybdenum, niobium and silicon, have been added individually and simultaneously in amounts of 0.1% to achieve solid solution strengthening. Silicon provides the highest potential for solid solution strengthening and, in addition, its melting point ($T_{M,Si} \approx 1414°C$) matches well to that of titanium ($T_{M,Ti} \approx 1688°C$) so that silicon can be added without the need of master alloys. Therefore, up to 0.4% of silicon have been used in the alloys.

The following alloy compositions have been produced and investigated: Ti 0.4O 0.5Fe 0.08C (base alloy), Ti 0.4O 0.5Fe 0.08C 0.1Au (gold addition to the base alloy), Ti 0.4O 0.5Fe 0.08C 0.1Mo (molybdenum addition to the base alloy), Ti 0.4O 0.5Fe 0.08C 0.1Nb (niobium addition to the base alloy), Ti 0.4O 0.5Fe 0.08C (0.1, 0.3, 0.5)Si (silicon addition to the base alloy in three different quantities), Ti 0.4O 0.5Fe 0.08C 0.1Au 0.1 Mo 0.1Nb 0.1Si (simultaneous addition of gold, molybdenum, niobium and silicon to the base alloy). Standard CP-Titanium Grade 4 (chemical composition Ti: balance, O: 0.29%, Fe 0.19%, C: 0.01%, H: 0.015%) and Ti 6Al 4V ELI (Ti balance, Al: 5.9%, V: 4.0%, O: 0.08%, Fe: 0.10%, C: 0.01%, H: 0.012%) have been used as reference materials.

Microstructure, Phase Composition and Mechanical Properties

After melting and casting, all alloys consisted of a fully martensitic α'-microstructure. This can be ascribed to the rapid cooling of the samples during casting. Stress relief annealed samples had equiaxed grains with an average grain size of approx. 100 µm (laboratory conditions). After hot-rolling and recrystallisation (larger quantities), in rolling direction slightly elongated grains have been observed, whereas equiaxed grains were visible in transverse direction. The grain size in transversal direction was reduced to about 25 µm. In addition, recrystallisation twins were visible.

In the recrystallized state, all alloys consisted of α- and transformed β-phase. In synchrotron radiation experiments, relatively low volume fractions of phases can be detected. Therefore, the presence of additional intermetallic compounds in any of the alloys can be practically excluded. Additions of the β-stabilizers in low amounts, i.e. 0.5% of iron, lead to the formation of a two-phase alloy by element partitioning. The mechanical properties of the different alloys investigated in our study are shown in Table 1. As can be seen, Ti 0.4O 0.5Fe 0.08C 0.3Si alloy has reached the mechanical properties of Ti 6Al 4V ELI. Therefore, larger quantities of this alloy will be produced and tested in the near future to finally get the new class of Al- and V-free Titanium alloys introduced into medical applications.

Table 1 – Hardness and tensile properties of the investigated alloys

alloy composition	hardness (HV10)	YTS (N/mm^2)	UTS (N/mm^2)	A (%)
Ti 0.4O 0.5Fe 0.08C	275[1)]	640[1)]	680[1)]	17[1)]
		650[2)]	750[2)]	16[2)]
Ti 0.4O 0.5Fe 0.08C 0.1Au	285[1)]	730[1)]	800[1)]	21[1)]
		740[2)]	820[2)]	20[2)]
Ti 0.4O 0.5Fe 0.08C 0.1Mo	295[1)]	780[1)]	800[1)]	19[1)]
Ti 0.4O 0.5Fe 0.08C 0.1Nb	290[1)]	780[1)]	800[1)]	22[1)]
Ti 0.4O 0.5Fe 0.08C 0.1Si	300[1)]	830[1)]	845[1)]	20[1)]
Ti 0.4O 0.5Fe 0.08C 0.3Si	310[1)]	910[1)]	920[1)]	18[1)]
Ti 0.4O 0.5Fe 0.08C 0.5Si	330[1)]	1010[1)]	1020[1)]	12[1)]
Ti 0.4O 0.5Fe 0.08C 0.1Au 0.1Mo 0.1Nb 0.1Si	305[1)]	865[1)]	875[1)]	17[1)]
CP-Titanium Grade 4	220[1)]	530[1)]	620[1)]	19[1)]
		483[3)]	550[3)]	15[3)]
Ti 6Al 4V ELI	310[1)]	895[1)]	930[1)]	16[1)]
		795[4)]	860[4)]	10[4)]

[1)] Material produced using laboratory conditions, tensile test results: average of two specimens.[2)] Material produced in larger quantities, tensile tests were carried out at flat specimens in rolling direction, average of three values. [3)] Minimal values specified in ASTM F67.[4)] Minimal values specified in ASTM F136.

FREE-MACHINING TITANIUM ALLOYS CONTAINING RARE EARTH METALS

Different experimental alloys based on Ti 6Al 4V, which is already used in automotive applications e.g. as fastener material, have been produced. Vanadium has partly been replaced by different ferromolybdenum pre-alloys or niobium to improve the ductility. In addition, low amounts of copper (known to enhance the deformability of titanium (Peters & Leyens, 2002)) and silicon (improving the castability as well as the oxidation and creep behavior (Lütjering & Williams, 2007)) were added to particular alloys. Finally, rare-earth metals were used for improved machinability. The alloy compositions tested in our study were: Ti 6Al 4V 0.9La/1.5La, Ti 6Al 4V 0.9Ce, Ti 6Al 4V 0.9Er (only rare-earth metal addition to Ti 6Al 4V), Ti 6Al 7Nb 0.9La (replacement of vanadium by niobium), Ti 6Al 2Fe 1Mo 0.9La, Ti 6Al 1Fe 2Mo 0.9La (replacement of vanadium by iron-molybdenum) Ti 6Al 2Fe 1Mo 0.9La 0.5Cu (copper addition) and Ti 6Al 2V 3Nb 0.9La 0.7Fe 0.3Si (optimized alloy composition).

Microstructure and Phase Composition

As the solvability of rare-earth metals in titanium is negligible at room temperature, the microstructure of all rare-earth-containing alloys after melting, casting and a solution treatment consisted of a titanium α'-matrix and discrete, equiaxed, metallic rare earth metal particles (identified by synchrotron diffraction) with a diameter between 2 µm and 20 µm in all 0.9% rare earth metal element containing alloys. Higher contents lead to a line-like decoration of the grain boundaries. The initial grain size was similar in all cases and lay between 50 µm and 150 µm. Thermo-mechanical treatments applied to the alloys neither changed the particle size nor the location of the particles in the microstructure. Therefore, the particle dissolution kinetics must be very slow as the microstructure did not change even after eight-hour heat treatments 200°C above β-transus temperature.

In most of the alloys, the particles were located mainly on the grain boundaries which can be explained as follows: The plasma during arc melting superheats the melt by about 30°C to 50°C only (Peters & Leyens, 2002). The melting point of titanium (1668°C) and the investigated alloys (between 1630°C and 1705°C) is larger than the melting temperature of all rare earth metals, namely, $T_{M,Ce}$ = 798°C, $T_{M,La}$ = 918°C and $T_{M,Er}$ = 1529°C, used. During cooling, the crystallization of the titanium matrix (containing the alloying elements) starts at the edges of the mold, grains form and only a limited number of rare earth metal atoms is dissolved in titanium. The remaining liquid phase must therefore be enriched in rare earth metal elements. Finally, once the matrix is fully crystallized, the remaining rare earth metals are trapped on the grain boundaries and crystallize during further cooling.

Machinability

During turning of Ti 6Al 4V long chips formed as expected. In case pure metallic cerium and lanthanum were present in the alloys, short chips formed. An example is given in Figure 2 showing chips of Ti 6Al 4V, Ti 6Al 4V 0.9La and Ti 6Al 4V 0.9Er alloys. It can be seen that short chips are produced only if pure metallic lanthanum is present. This observation can be explained as follows: During segmented chip formation the temperature in the shear bands reaches or exceeds 1000°C (Siemers, Bäker, Mukherji & Rösler, 2003). Metallic lanthanum particles which are present in the zone of localized deformation will drastically soften or even melt once the segment (and the shear band) starts to form. The adhesion between the segments will then be reduced so that the chips fall apart either directly once the shear band forms or due to vibrations during further progress of the tool after the segment is completely developed. This explanation is promoted by strongly elongated lanthanum particles being found on some of the shear planes and the fact that most of the chips of the lanthanum containing alloys were separated in the primary shear zones (Rösler, Bäker, Siemers, 2008). Consequently, the addition of erbium cannot lead to short chips as the melting point of erbium is much higher than the temperatures reached during the shear band formation.

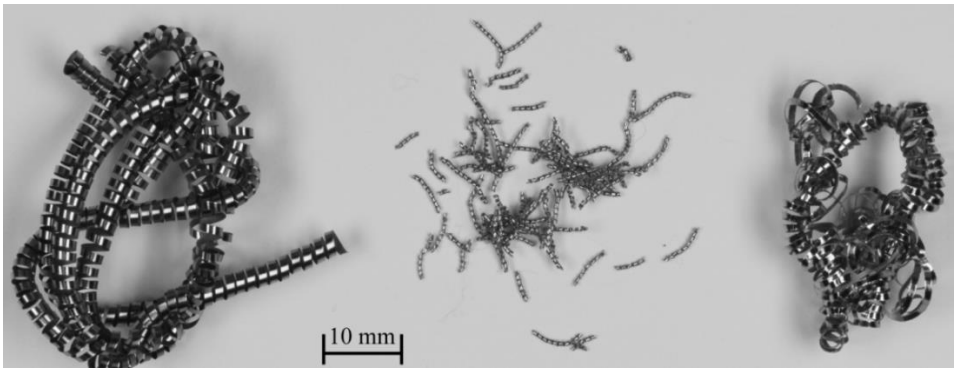

Figure 2 – Chips of Ti 6Al 4V (left), Ti 6Al 4V 0.9La (centre) and Ti 6Al 4V 0.9Er alloys (right).

Mechanical Properties

At room temperature, the tensile strength of the lanthanum containing Ti 6Al 4 0.9La alloy was about 8% higher compared to the standard alloy, whereas the ductility was diminished by about 30%. On the one hand, the grain refinement caused by the lanthanum particles lead to strengthened alloys. On the other hand, the particles weakened the grain boundaries and cracks could propagate easier. The yield tensile strength, the ultimate tensile strength and especially the minimal elongation at rupture (Ti 6Al 4V 0.9La: 10.5%) of the industrially produced material fulfilled the requirements of ASTM B348 for Ti 6Al 4V alloy. The Ti 6Al 4V 0.9La industrially processed material showed a fatigue limit of about 550 MPa (at $R \approx 0.01$). The lanthanum particles had a negative effect on the fatigue properties as they acted as crack initiating points. The fatigue limit of the standard alloy Ti 6Al 4V was 600 MPa (at $R \approx 0.01$) which was about 10% higher compared to the lanthanum containing alloys. Biocompatibility, corrosion resistance and the physical properties were similar (Feyerabend, Siemers, Willumeit, Rösler, 2009). Even if Ti 6Al 2V 3Nb 0.9La 0.7Fe 0.3Si showed better mechanical properties, i.e. higher ductility, compared to Ti 6Al 4V 0.9La, all the lanthanum modified alloys should preferably be applied in non-safety critical applications, e.g. in the automotive industry.

ACKNOWLEDGEMENTS

The authors thank our colleagues from the BTU Cottbus (S. Bolz and D. Domke) and from Access e.V. (R. Tiefers) for the alloy production in larger quantities and U. Ruett and O. Gutowski for the assistance during the experiments at beamline P07 (PETRA III) of HASYLAB, DESY in Germany.

REFERENCES

Boyer, R., Welsh, G. & Collings, E.W., Eds. (1994). *Materials properties handbook: titanium alloys*. Ohio, USA: ASM International.

Boyer, R., Williams, J.C. (2012). Developments in Research and Applications in the Titanium Industry in the USA. In: Zhou, L., Chang, H., Lu, Y., Xu, D. (Eds.), *Twelfth World Conference on Titanium* (pp. 10-19), Beijing, China: Science Press Beijing.

Donarchie, J., Ed. (1988). *Titanium – a technical guide*. Metals Park, Ohio, USA: ASM International.

Geetha, M., Singh, A.K, Asokamani, R. & Gogia, A. (2009), Ti based biomaterials, the ultimate choice for orthopaedic implants – A Review, *Progress in Materials Science*, *54*, 397-425.

Feyerabend, F., Siemers, C., Willumeit, R & Rösler, J. (2009). Cytocompatibility of a free machining titanium alloy containing lanthanum, *Journal of Biomedical Materials Research Part A, Vol 90A, Issue 3*, 931-939.

Fox, S. & Yu, K.O. (2012). Recent Changes and Developments in Titanium Extraction. In: Zhou, L., Chang, H., Lu, Y., Xu, D. (Eds.), *Twelfth World Conference on Titanium* (pp. 65-71), Beijing, China: Science Press Beijing.

Hammersley, A.P., Svensson, S.O., Hanfland, M., Fitch, A.N. & Häusermann, D. (1996). Two dimensional detector software: from real detector to idealised image or two theta scan, *High Pressure Research, 14 (4-5)*, 235-248.

Healy, C., Koch, S, Siemers, C., Mukherji, D. & Ackland, G.J. (2015). Shear melting and high temperature embrittlement: Theory and application to machining titanium, *Physical Review Letters 114 (16)*, 165501.

Hench, L.L. & Polak, J.M (2002).Third-Generation Biomedical Materials, *Science, 8 (295 no 5557)*, 1014-1017.

Hou, Z.B. & Komanduri, R. (1997). Modelling of thermomechanical shear instability in machining. *International Journal of Mechanical Sciences*, 39 (11), 1273-1314.

Lütjering, G. & Williams, J.C. (2007). *Titanium*. Berlin, Germany: Springer.

Mabilleau, G, Bourdon, S., Joly-Guillou, M.L., Filmon, R., Baslé, M.F., & Chappard, D. (2006). Influence of fluoride, hydrogen peroxide, lactatic acid on the corrosion resistance of commercially pure titanium, *Acta Biomaterialia, 2*, 121-129.

Maki, K., Shioda, M. & Sayashi, M. (1992). Effect of silicon and niobium on oxidation resistance of TiAl intermetallics, *Materials Science and Engineering: A, Volume 153 (1-2)*, 591-596.

Mitsuo, A., Uchida, S., Nihira, N., Iwaki, M. (1998). Improvement of high-temperature oxidation resistance of titanium nitride and titanium carbide films by aluminum ion implantation, *Surface and Coatings Technology, 103-104*, 98-103.

Ng, H.P., Douguet, E., Bettles, C.J. & Muddle, B.C. (2010). Age-hardening behaviour of two metastable beta-titanium alloys, *Materials Science and Engineering A 527*, 7017-7026.

Okano, H., Hatta, Y., Tada, O. & Tanaka, H. (2007). Titanium ingot production at Toho Titanium Co., Ltd. In: M. Niinomi, S. Akiyama, M. Hagiwara, M. Ikeda & K. Maruyama (Eds.), *Eleventh World Conference on Titanium* (pp. 155-158), Kyoto, Japan: The Japan Institute of Metals.

Peters, M. & Leyens, C., Eds. (2002). *Titanium and titanium alloys*. Weinheim, Germany: Wiley-VCH.

Rösler, J., Bäker, M. & Siemers, C. (2008) European Patent No EP 1644158. Munich, Germany: European Patent Office.

Schell, N., King, A., Beckmann, F., Ruhnau, H. U., Kirchhof, R., Kiehn, R., Mueller, M. & Schreyer, A. (2009). The High Energy Materials Science Beamline (HEMS) at PETRA III. In: Garrett, R., Gentle, I., Nugent, K. & Wilkins, S (Eds.), *10th International Conference on Synchrotron Radiation Instrumentation* (pp. 391-394), Melbourne, Australia: The American Institute of Physics.

Siemers, C., Laukart, J., Roesler, J., Rokicki, P. & Saksl, K. (2011). Advanced titanium alloys containing micrometer-size particles. In: Zhou, L., Chang, H., Lu, Y. & Xu, D (Eds.), *Proceedings of the twelveth World Conference on Titanium* (pp. 883-887), Beijing, China: The Nonferrus Metals Society of China.

Siemers, C., Laukart, J., Zahra, B., Rösler, J., Spotz, Z., & Saksl, K. (2010). Development of advanced and free-machining titanium alloys. In: D. Gallienne, M. Bilodeau (Eds.) *Fortynineth Conference of Metallurgists, Section Light Metals 2010 - Advances in Materials and Processes* (pp. 311-322), Vancouver, Canada: The Canadian Institute of Mining, Metallurgy and Petroleum.

Siemers, C., Jencus, P., Baeker, M., Roesler, J. & Feyerabend, F. (2007). A new free machining titanium alloy containing lanthanum. In: M. Niinomi, S. Akiyama, M. Hagiwara, M. Ikeda & K. Maruyama (Eds.), *Eleventh World Conference on Titanium* (pp. 709-712). Kyoto, Japan: The Japan Institute of Metals.

Siemers, C., Bäker, M., Mukherji, D. & Rösler, J. (2003). Microstructure evolution in shear bands during the chip formation of Ti 6Al 4V. In: G. Lütjering & J. Albrecht (Eds.). *Tenth World Conference on Titanium* (pp. 839-846). Hamburg, Germany: Wiley VCH.

Toby, B.H. (2005). CMPR - a powder diffraction toolkit. *Journal of Applied Crystallography, 38*, 1040-1041.

Tegner, B.E., Zhu, L., Siemers, C., Saksl, K. & Ackland, G.J (2015). High temperature oxidation resistance in Titanium-Niobium Alloys, *Journal of Alloys and Compounds, 643*, 100-105.

Tönshoff, H.K. & Hollmann, F., Eds. (2005). *High Speed Machining*. Weinheim, Germany: VCH-Wiley.

Yokel, R.A., Allen, D.D. & Ackley, D.C. (1999). The distribution of aluminum into and out of the brain, *Journal of Inorganic Biochemistry, 76*, 127-132.